Research Reviews: Journal of Material Science

DOI: 10.4172/2321-6212.1000193

e-ISSN: 2321-6212
p-ISSN: 2347-2278
www.rroij.com

Difference in the Mechanism of Electrochemical Deoxidation of Conducting and Non-conducting Solid Oxide Preforms: An Experimental Demonstration with TiO_2 and SiO_2 Pellet Electrodes in $CaCl_2$ Melt

Sri Maha Vishnu D[1,2*], Sanil N[1] and Mohandas KS[1]

[1]Chemistry Group, Indira Gandhi Centre for Atomic Research, Kalpakkam-603102, India

[2]Materials Chemistry Group, Department of Materials Science and Metallurgy, University of Cambridge, Cambridge CB3 0FS, UK

[*]**For Correspondence:** Sri Maha Vishnu D, Materials Chemistry Group, Department of Materials Science and Metallurgy, University of Cambridge, Cambridge CB3 0FS, UK, Tel.: +44 (0) 1223 334300; Fax: +44 (0) 1223 334567; E-mail: smvd2@cam.ac.uk

Received date: Mar 27, 2017, **Accepted date:** Sep 18, 2017, **Published date:** Oct 09, 2017

Research Article

ABSTRACT

Powder compacted and sintered solid oxide preforms, generally shaped as thin pellets, have been used as the negative electrode of a molten salt electro-deoxidation cell and deoxidation of the electrode is greatly influenced by its electrical conductivity. The deoxidation pattern of electron conducting and non-conducting oxide preforms should, therefore, be different. In order to demonstrate this experimentally, novel electrochemical experiments were carried out with electron conducting TiO_2 and non-conducting SiO_2 pellet electrodes in calcium chloride melt at 1173 K. The experimental results have shown, as already reported by many previously, that three physically distinct phases, viz. the solid electron conductor, the oxide and the electrolyte melt should coexist for electro-deoxidation of non-conducting SiO_2 electrode but only two physically distinct phases, viz. the oxide and the electrolyte melt need only to coexist in the case of conducting TiO_2 electrode. It is demonstrated in this study, for the first time, that the 3 Phase Interline (3PI) mechanism, proposed to explain electro-deoxidation of solid oxides in general, stands reduced to 2 Phase Interface (2 PI) mechanism in the case of conducting oxides.

Keywords: Electrical conductivity, Solid state electrochemical deoxidation, Titanium dioxide, Silicon dioxide, Calcium chloride, 3 PI mechanism

INTRODUCTION

Direct electrochemical reduction of oxides in the solid state to corresponding metals or elements using molten salts as the electrolyte medium is a recent development in electrometallurgy and significant R&D work has been reported in this field of study [1-3]. Conventionally, the metal production technologies are based on either chemical methods (e.g., metallothermic, carbothermic reduction) or electrochemical methods (in which the metal is produced cathodically from an electrolyte solution containing the metal in dissolved form, e.g., Hall-Heroults' process for the production of aluminium) [4]. Due to the inherent limitations and difficulties in the existing technologies for metals production, new methods offering advantages such as low temperature of operation, less number of process steps, higher energy efficiency, environment friendliness etc. are of interest to conventional metallurgical industries for the production of metals. In this context, the direct oxide electrochemical reduction method, called the FFC Cambridge process [2,3], is of interest.

In FFC Cambridge process [2,3], the electro-deoxidation of the oxide is carried out by configuring it as the cathode against graphite counter electrode in a cell in which molten $CaCl_2$ at ~1173 K is generally employed as the electrolyte. The solid oxide preform will be in physical contact with a metal part, which acts as the conduit for electrons between the external power supply and the oxide electrode. When an appropriate potential, generally 3.0 or 3.1 V, is applied between the electrodes and sufficient time is given for the electrodeoxidation process to go to completion, the metal oxide cathode is transformed to the corresponding metal. The overall cathodic reaction can be represented as,

$$MO_2 + 4e^- = M + 2O^{2-} \quad (1)$$

e-ISSN: 2321-6212
p-ISSN: 2347-2278

Where MO_2 is the metal oxide and M is the corresponding metal. The O^{2-} ions dissolve in the electrolyte melt and are transported to the graphite anode where they discharge to form CO_2 gas as

$$2O^{2-} + C = CO_2 + 4e^- \quad (2)$$

Reaction (1) shows that electrons are the reductant in the electro-reduction process and hence presence of those at the reaction interface of the oxide particle is very important for deoxidation to occur. The cathodically generated O^{2-} ions are required to be dissolved in the melt and transported to the anode for discharge as per reaction (2) and hence the presence of the electrolyte melt at the reaction interface becomes another essential condition of the electro-deoxidation process. The co-existence of three components, viz. the oxide, electron and electrolyte melt at the reaction interface thus becomes the necessary and essential condition for the electrochemical deoxidation of a solid oxide in an electrolyte medium. A solid metal part will be in close physical contact with the oxide preform through which the electrons from an external DC power source will be supplied to it. The thermodynamic stability and electrical characteristics of an oxide electrode are known to have strong influence on its electro-reduction behaviour [3,5,6] in addition to many other parameters such as applied voltage, duration of electrolysis, sintering temperature of the oxide performs etc. [3,7,8]. Several studies have been reported on the electrochemical reduction of oxides such as TiO_2 [1,3,5,8-11], Nb_2O_5 [7,12,13], UO_2 [14-16], SiO_2 [17-26] etc. The process is being pursued in view of production of solar grade silicon as well [27].

Chen et al. [28] proposed 3 phase interline (3 PI) mechanism to explain the initiation and propagation of electro-deoxidation in a solid oxide preform in molten salt medium. In this mechanism, the reduction starts at the solid electron conductor-oxide-melt three phase interlines and the freshly formed metal acts as the bridge to conduct electrons to the adjoining oxide particles so as to form new interlines for propagation of deoxidation throughout the solid matrix. Obviously, the oxide is considered as a non-conductor of electrons in this mechanism so that a separate physical phase (solid metal electron conductor) is required to be present at the reaction interface to make available the electrons necessary for the electrodeoxidation reaction (1) to occur. This situation demands the co-existence of the three physically distinct phases (the solid electron conductor, the oxide and electrolyte melt) at the reaction interface. However, if the oxide is a good conductor, a separate third phase, i.e. the solid electron conductor at the reaction interface may seem unnecessary and in that case the electrodeoxidation of the oxide can be expected to follow a 2-phase interface (2PI) mechanism.

Many studies have been reported on the direct electrochemical deoxidation of insulating SiO_2 in calcium chloride melt and the results show that the electrodeoxidation of the solid electrode proceed via. the 3PI mechanism explained above [17-22,27,28]. The initiation-expansion-shrinking-disappearance (IESD) process of the solid (conductive product)/solid (oxide)/liquid (electrolyte) three-phase reaction boundary (TPB), proposed to explain the electro-deoxidation of insulating compounds [29], fits well with the deoxidation pattern of insulating SiO_2 preforms [23,30-33]. Though several such reports are available on the 3PI mechanism of electrodeoxidation of insulating oxides with SiO_2 as the typical example, no study has yet been reported, to the best of our knowledge, which brings out the difference in the mechanism of electrodeoxidation of conducting and non-conducting oxides. Instead, the discussions on this subject in the literature often present an impression that the 3 PI mechanism of electrodeoxidation is a general one and it can explain the initiation and propagation of electrodeoxidation in all kinds of oxide preforms.

Hence it is the aim of this study, to experimentally demonstrate the difference between the electrodeoxidation mechanism between electrically conducting and non-conducting oxide electrodes and thus to give experimental proof to our new proposal of 2PI mechanism of electro-deoxidation of conducting oxides. For reasons stated below, TiO_2 and SiO_2 have been selected as the conducting and non-conducting oxides respectively for the present study. Electrodeoxidation of both the oxides has been studied in detail and reported by many groups in the past fifteen years and hence it is not the purpose and aim of this study to re-investigate such of those aspects of electrodeoxidation of the two oxides. The present experiments are designed only with the limited aim of driving home the difference in the physical mechanism of propagation of electrodeoxidation between the conducting and non-conducting oxides. The details of the study are reported in this article.

Electrical conduction properties of solid TiO_2 and SiO_2

TiO_2 and SiO_2 belong to two distinctly different classes of oxides with respect to their chemical and electrical properties. Phase diagram of the Ti-O [34] system shows the existence of different sub-oxides and sub-stoichiometric phases called magnelli phases (Ti_nO_{2n-1} where $4 < n < 10$) to TiO_2. The multiple valence of Ti makes electrical conduction in the Ti-O system possible. The Magnelli phases are high conducting and hence removal of small amount of oxygen from stoichiometric TiO_2 electrode, by cathodic polarisation in an electro-deoxidation cell or otherwise, could make it electronically conducting. TiO_2 is a semiconductor and its electrical properties also changes with the oxygen partial pressures [35]. The electro-reduction of TiO_2 in $CaCl_2$ melt is known to proceed via formation and decomposition of Ca-Ti-O intermediate compounds and sub-oxides of Ti [9], which also possess good electrical conductivity [36]. All these enable the solid electrode to remain electrically conducting throughout the course of its electro-deoxidation to titanium metal in

e-ISSN: 2321-6212
p-ISSN: 2347-2278

the electro-reduction cell. On the other hand, the Si-O system [37] does not show the existence of any sub-oxides to SiO_2. So, electron conduction on account of variable valence of silicon is not possible in a SiO_2 pellet electrode. Also, the large band gap (>5 eV) between the valence and conduction bands in SiO_2 makes it a very poor electronic conductor (the conductivity of SiO_2 is reported to be in the range of 10^{-11}-10^{-9} $\Omega^{-1}cm^{-1}$ in the temperature range 1073-1223 K) [38]. In short, solid TiO_2 and SiO_2 preforms will function as electron conducting and non-conducting electrodes respectively in a high-temperature molten salt electro-deoxidation cell.

EXPERIMENTAL SECTION

Moisture-free $CaCl_2$ was obtained by thermal drying of $CaCl_2.6H_2O$ (Merck, Extra Pure) under vacuum as discussed [7]. The dried salts were stored in an inert atmosphere glove box prior to use in the experiments. TiO_2 (rutile, >98% purity, Rankem, India) and SiO_2 (>99.5% purity, Alfa Aesar) powders were thoroughly mixed with 1 wt.% polyvinyl alcohol and 0.5 wt.% polyethylene glycol and made a slurry in isopropyl alcohol, which was then dried under an IR lamp. The solid mass was finely powdered by using a mortar and pestle and uniaxially pressed into pellets. The pellets were sintered at 1573 K for 3 hours. All the experimental parameters were maintained more or less similar during preparation of the pellets so as to enable comparison of their electro-reduction behavior. The open porosity of the TiO_2 and SiO_2 pellets was measured by using Archimedes principle and found to be ~20% and ~40%, respectively.

The pellets were employed as cathodes in two different configurations in the electro-reduction cell as shown in **Figure 1a and 1b**. In one configuration, a 2 mm dia. hole was drilled at the centre of the pellet and a tantalum wire, which acted as current lead to the oxide pellet, was connected to it and the whole pellet with the associated metal part was immersed in the melt. In the other configuration, the hole was drilled near the edge of the pellet, through which the current collector tantalum wire was tied. In this configuration, the pellet was dipped in the melt in such a way that it alone was in contact with the melt and not the metal current collector (**Figure 1b**). Graphite rods (10 mm dia., 100 mm long, supplied by M/s. Nickunj Group, Mumbai) were employed as the counter electrode during electrolysis and cyclic voltammetric studies of the solid oxide electrode. A Ni/NiO couple was used as the reference electrode in the above measurements.

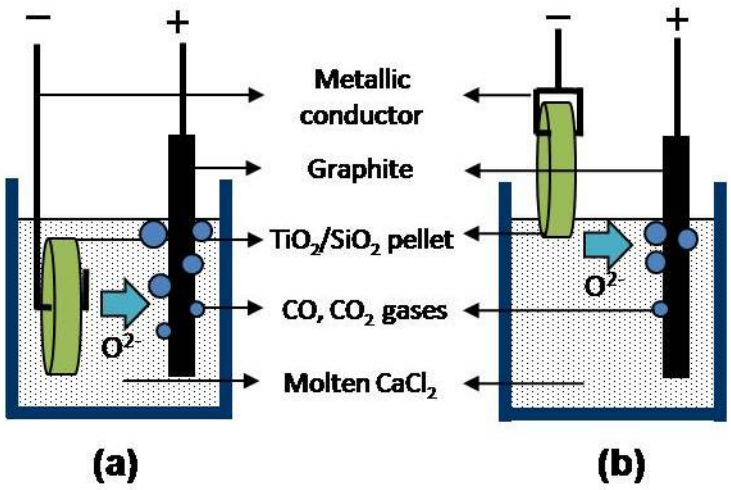

Figure 1. The schematic of the electro-deoxidation cell with two configurations of the oxide pellet electrode, (a) pellet immersed fully in melt and (b) the tip of the pellet alone in contact with the melt.

An alumina crucible was used to contain the salt and it was placed in a stainless steel reactor vessel. The assembly of the reactor vessel with all the electrodes in place was carried out in an argon atmosphere glove box. The details of the cell-assembly are given [5]. After assembly, the cell was brought outside and heated to 1173 K with the help of a resistance heating furnace. High purity argon was passed through the reactor throughout the course of the experiments. The melt was pre-electrolysed at 2.8 V until the background current attained a stable minimum value. Cyclic voltammetry was carried out in the melt with tungsten wire (1 mm dia.) and the tip of the oxide pellets as the working electrodes (WE). Electrolysis of the oxides, in both the configurations as shown in **Figure 1a and 1b**, was carried out at a constant voltage of 3.1 V for 22 h by using a DC power supply (M/s Digitronics, Chennai).

After completion of electrolysis, the products were recovered from the cell, washed thoroughly, dried under vacuum and subjected to XRD analysis by using a PANalytical 1011 X-ray diffractometer. The microstructural changes and elemental composition of the samples were studied using a scanning electron microscope (SEM, Philips model XL 30) coupled with an energy dispersive X-ray analyser (EDX). The oxygen analysis of the samples was carried out by using ELTRA ONH2000 oxygen/nitrogen analyser.

e-ISSN: 2321-6212
p-ISSN: 2347-2278

RESULTS AND DISCUSSION

Cyclic Voltammetry of Tungsten and TiO_2 in $CaCl_2$ Melt

The cyclic voltammograms obtained with the tip of a tungsten wire and the tip of a TiO_2 pellet as the working electrodes (WEs) (**Figure 1b**) in separate CV experiments with graphite rod as the counter electrode (CE) in $CaCl_2$ melt at 1173 K are given in **Figure 2**. The CV of the tungsten wire electrode (curve 1) shows that the reversible calcium deposition potential of the melt occurs at 0.00 V vs Ca/Ca^{2+}. With the edge of TiO_2 pellet as WE (configuration as given in **Figure 1b**, initial few CVs did not show any characteristic electrochemical features of the electrode and the CVs looked similar to that of a resistor (curve 2). However, upon repeated cycling of the electrode in the potential band +1.5 V-0.0 V, a reduction current wave appeared at ~+0.5 V vs. Ca/Ca^{2+} (curve 3) suggesting thereby that the electrode was made electrochemically active by the potential cycling in the melt. The fact that the CV could be performed on the $TiO_2/CaCl_2$ melt/graphite cell proved that the cell circuit was closed and the TiO_2 electrode was electronically conducting in the given configuration of the electrode. Identical CV experiments were attempted with SiO_2 pellet electrodes (configuration as in **Figure1b**, immediately after it was allowed to be in contact with the melt, but it was not possible to record CV as the cell was open. The cell behaviour showed that, unlike TiO_2, the SiO_2 pellet was not electronically conducting.

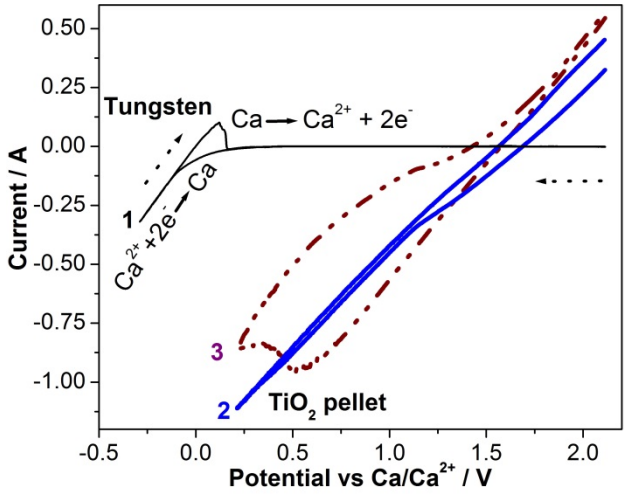

Figure 2. Cyclic voltammograms obtained with the tip of a 1mm dia. tungsten wire (labeled 'Tungsten', curve 1) and the edge of a TiO_2 pellet (two curves labeled as 'TiO_2 pellet') as the working electrodes in $CaCl_2$ melt at 1173 K. Scan rate: 20 mV/s. Several successive scans were performed with TiO_2 pellet electrode and the CVs of 1st and 11th scans are shown in the figure as curve 2 and curve 3 respectively.

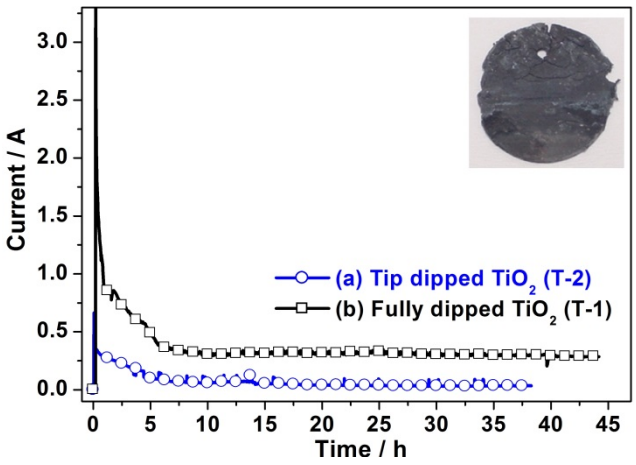

Figure 3. Current variation during electrochemical reduction of TiO_2 pellet in the (a) Tip dipped (T-2) and (b) fully dipped (T-1) configurations at 3.1 V in $CaCl_2$ melt at 1173 K.

Electro-reduction of TiO_2 Pellets in $CaCl_2$ Melt

The electrolysis curves (I-t curve) obtained with two TiO_2 pellets, one each in the two configurations given in **Figure 1a and 1b**, are shown in **Figure 3**. The photograph of the TiO_2 pellet after electrolysis in the 'tip alone contact' configuration is given as inset in the figure. The pellet was sectioned in to three parts along its vertical length as top (T), middle (M) and

e-ISSN: 2321-6212
p-ISSN: 2347-2278

bottom (B) parts. XRD patterns of the powdered samples from the three parts are given in **Figure 4a-4c** The different chemical phases identified in the three samples are given in the respective figures. For comparison, XRD pattern of the TiO_2 pellet electrolysed in fully dipped condition is given in **Figure 4d**, which showed that the oxide is completely converted to Ti metal.

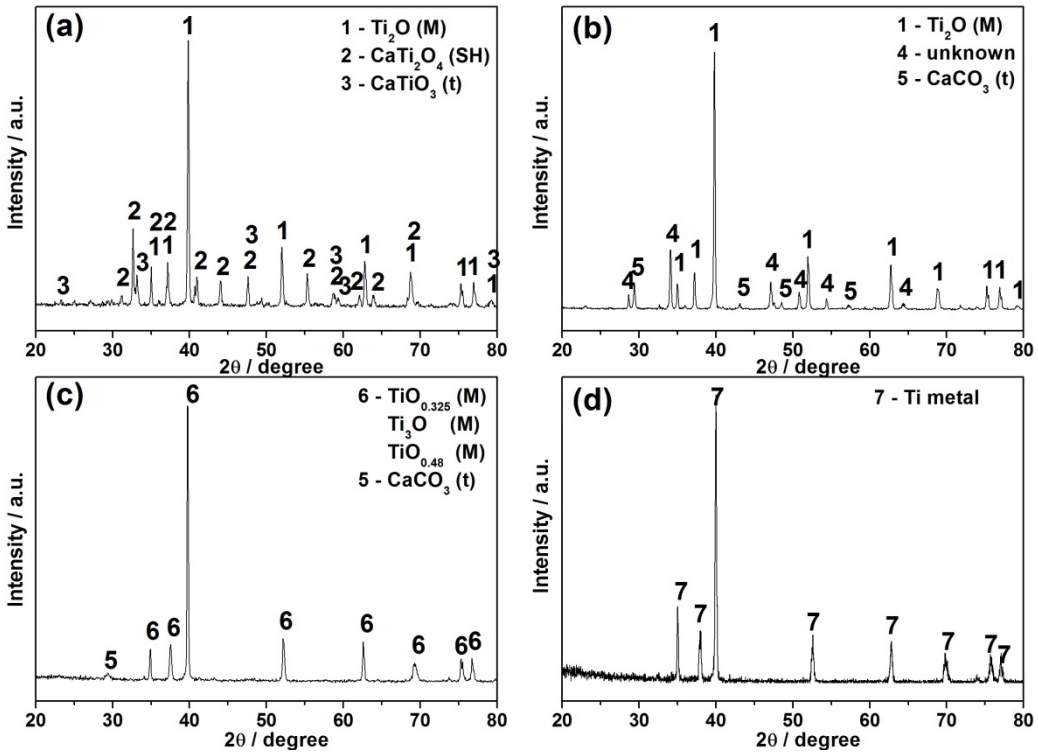

Figure 4. XRD patterns of the uniformly ground powders from (a) Top, (b) middle and (c) bottom regions of the TiO_2 pellet, polarised cathodically in the 'tip alone in contact' configuration and (d) uniformly ground pellet electrolysed in full dipped condition.

Schwandt and Fray [9] reported that TiO_2 solid electrode undergoes multiple reactions and phase changes during its conversion to Ti metal in $CaCl_2$ melt. A simple reduction scheme with the sequence of reactions could be deduced from the study as $TiO_2 \rightarrow Ti_4O_7+CaTiO_3 \rightarrow Ti_3O_5+CaTiO_3 \rightarrow Ti_2O_3+CaTiO_3 \rightarrow CaTi_2O_4+TiO \rightarrow Ti_2O \rightarrow Ti_3O \rightarrow Ti_6O \rightarrow Ti$. The chemical phases identified in the XRD analysis, therefore, show that both the top (a) and middle (b) parts of the pellet, were partially deoxidized (titanium oxides of lower valency and calcium titanates) and the bottom part (c) was completely deoxidized to titanium metal.

It is obvious that these chemical phases were formed by electrochemical reactions. The results make it clear that electrodeoxidation reactions, though in different extents, took place throughout the body of the pellet irrespective of the location of the electron supplying current lead to it. The typical nodular grains of titanium metal seen in the SEM image of the fractured surface of the melt dipped bottom part of the pellet (**Figure 5**) is in line with the XRD results and both results together confirm that the bottom part of the pellet, which was far away from the electron supplying metal wire contact to the pellet was reduced to titanium metal. It can also be noticed from the XRD results that no metal phase was present between the melt dipped bottom part of the oxide pellet and the tantalum current lead connected at the top through which electrons could have passed to the reduce the bottom part. Obviously, the electrons from the tantalum current lead, connected at the top edge of the pellet, reached the bottom melt dipped part by conduction through the body of the pellet. As seen from the XRD results, the pellet body through which the electrons were to be conducted to the bottom part was converted to lower oxides of titanium and calcium titanates by electrolysis. The fact that the bottom part of the pellet was reduced to Ti metal should, therefore, mean that not only TiO_2 but also the intermediate phases formed during the electrodeoxidation were good electronic conductors.

It becomes amply clear from the above results that the bottom part of the pellet was reduced to Ti metal in the absence of a solid metal electron conductor at the reaction interface and the electrons from the current lead were conducted to the reaction interface through the pellet body itself. It is obvious that the reduction reaction occurred at those locations of the pellet where the three components, i.e. the oxide, electron and melt necessary for reduction coexisted.

As the oxide pellet itself acted as the electron conductor, no separate and distinct physical phase was necessary for supply of electrons to the reaction interface, which reduced the number of co-existing physical phases from three to two (the oxide and melt). Thus the experimental results gave ample evidence that two physically distinct phases, i.e. the oxide

e-ISSN: 2321-6212
p-ISSN: 2347-2278

and melt need only coexist for electrodeoxidation of a conducting oxide like TiO_2 to occur and not three as required by the 3 PI mechanism of electro-deoxidation [28,32,33].

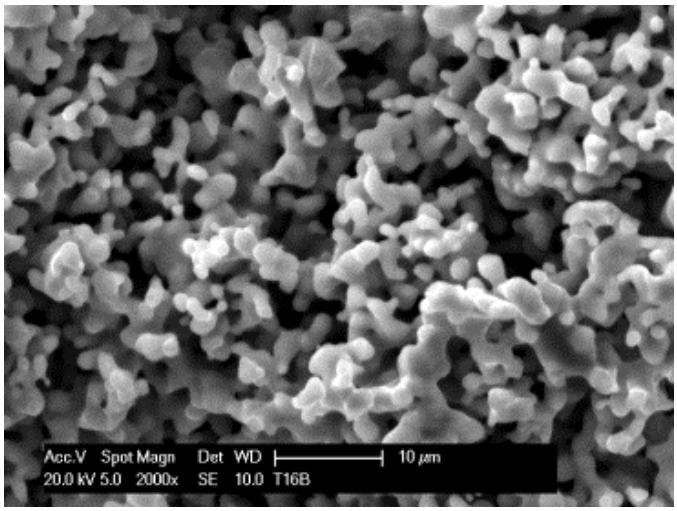

Figure 5. The SEM image of the fractured surface of the bottom (B) part of the electrolysed pellet shown in **Figure 3**. The typical nodular grains show that the oxide was converted to Ti metal.

As seen from the XRD analysis, the 'middle' and 'top' portions of the electrolysed pellet, which were not in physical contact with the electrolyte melt, were partially reduced. As the reduction of the oxide electrode was not possible without its physical contact with the electrolyte melt, the presence of melt at both 'M' and 'T' areas of the electrode becomes apparent. It is highly likely that the melt from bottom part of pellet seeped upwards through the pores in the pellet by capillary action and wetted the upper parts so that those areas too could be reduced.

The observed lower extent of reduction of the two parts (M and T) compared to the bottom melt dipped part should mean that reduction of the former areas were slowed down due to inadequacy of the molten electrolyte around these locations of the pellet. In the absence of sufficient quantity of electrolyte, the CaO produced during the initial reactions could have accumulated at those locations of the pellet and retarded the subsequent deoxidation reactions.

Electro-reduction of SiO_2 Pellets in $CaCl_2$ Melt

The results of identical experiment carried out with a SiO_2 pellet (mass: 1.5 g, 25 mm dia., 2 mm thick, open porosity 40%) in the $CaCl_2$ melt are discussed in this section.

As expected from the CV results, in the 'tip alone contact' configuration, the SiO_2 pellet was not conducting and hence current could not be passed through the graphite/melt/SiO_2 cell initially. However, after about 10 minutes, the continuity signal of the cell circuit could be obtained, but with a high resistance as shown by the multimeter. Obviously, the melt seeped through the pellet and reached the current lead, which helped to close the cell electrical circuit. Subsequently electrolysis was carried out at 3.1 V for 22 h.

Unlike in the case of the TiO_2 pellet, the SiO_2 pellet showed visibly distinct regions (shown by the dotted lines) along the vertical length of the pellet as positioned in the cell (**Figure 6b**). The pellet was sectioned along the dotted lines shown on the photograph (**Figure 6b**) and assigned the names (B), (M) and (T) to represent the bottom, middle and top parts. The XRD patterns of the powdered sample of the three parts are given in **Figure 7.**

The powder samples are quite distinguishable with their unique colours. Interestingly, as revealed by XRD data, the bottom melt dipped part was not reduced and remained as SiO_2. Significant microstructural changes have been observed in various regions of the pellet electrolysed in tip dipped condition in $CaCl_2$ melt, as could be seen from the microstructures given in **Figure 8**. The cross section of the dark yellow intermediate region of the pellet whose thickness was about ~1.5 mm, electrolysed in tip dipped condition was found to have columnar morphology with length of the grains being of the order of ~50 µm (**Figure 8b**) when compared to that of the pellet before electrolysis (**Figure 8a**). EDX analysis of the cross section (**Figure 8c**) showed an elemental profile containing Ca, Si and O and the region contained $CaSiO_3$ as the major phase as analysed by XRD.

In the light of the discussions made above on a similar experiment with TiO_2 pellet, it becomes quite clear that electrons could not be conducted through the SiO_2 pellet and hence the bottom area of the pellet, though dipped in the electrolyte, could not be reduced. However, the area of the pellet near the current collector wire where electrons could be supplied directly to the SiO_2 particles from the current collector, was found reduced to silicon as revealed by XRD analysis.

e-ISSN: 2321-6212
p-ISSN: 2347-2278

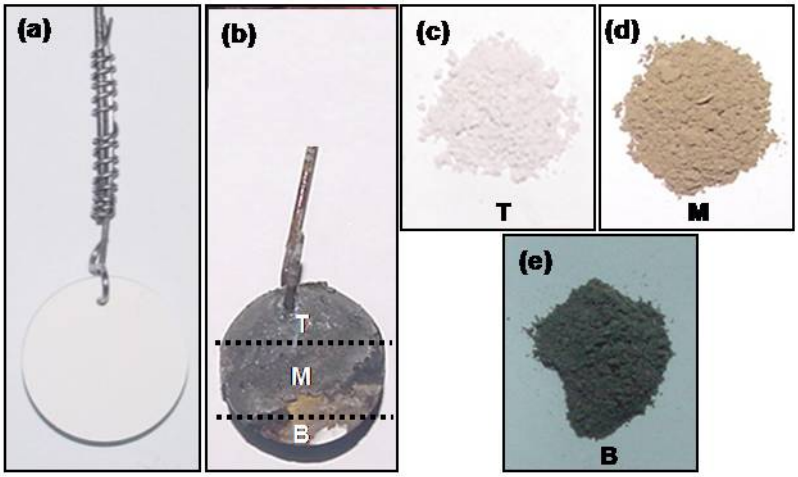

Figure 6. Photographs showing a SiO_2 pellet (a) before and (b) after electrolysis used in the tip alone contact configuration in $CaCl_2$ melt. The three visibly different parts of the electrolysed pellets, as marked by the dotted lines and labeled as the bottom (B), middle (M) and top (T) regions in (b) were separated and ground to powders and shown in the photographs (c), (d) and (e) respectively.

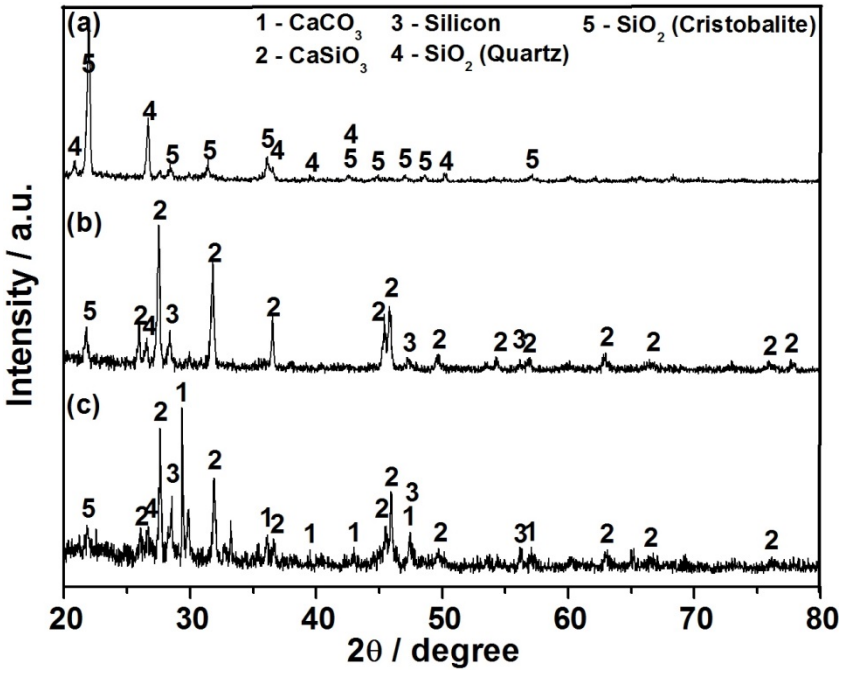

Figure 7. X-ray diffractograms of the powders from the (a) bottom (b) middle and (c) top portions of the pellet, corresponding to **Figure 6c-6e**. The phases are represented by: 1) $CaCO_3$, 2) $CaSiO_3$, 3) Si, 4) SiO_2 (quartz), 5) SiO_2 (cristobalite).

Identical results were reported earlier by Nohira et al. [23], during cathodic polarization of a quartz plate in $CaCl_2$ melt. The experimental results prove beyond any doubt that, unlike electron conducting TiO_2, the presence of an electron supplying solid electron conductor is essential at the reaction interface for electrodeoxidation of the insulating SiO_2 to occur. The 3PI mechanism of electrodeoxidation of insulating oxides, reported in many studies as mentioned previously, stands confirmed once again with the present experimental results.

Intermediates during the Electrochemical Reduction of TiO_2 versus SiO_2 Pellets

To further gain insight, TiO_2 and SiO_2 pellets each were electrolysed in $CaCl_2$ melt at applied cell voltages of 2.5 V and 2.8 V in separate experiments. The product of electrolysis in case of TiO_2 was found to contain various ternary intermediates and suboxides of Ti whereas silicon was the end product of electrolysis (**Figure 9a and 9b**) at both the voltages. In case of TiO_2, the partially reduced products contained $CaTiO_3$, $CaTi_2O_4$ and various suboxides. As the mechanism of reduction of TiO_2 and the reaction intermediates observed in the present study are similar to those reported by Schwandt and Fray [9], a detailed discussion on this aspect has been omitted. The SEM images of the silicon obtained from electrolysis of SiO_2 at 2.5 V and 2.8 V are given in **Figure 9c and 9d**, respectively.

e-ISSN: 2321-6212
p-ISSN: 2347-2278

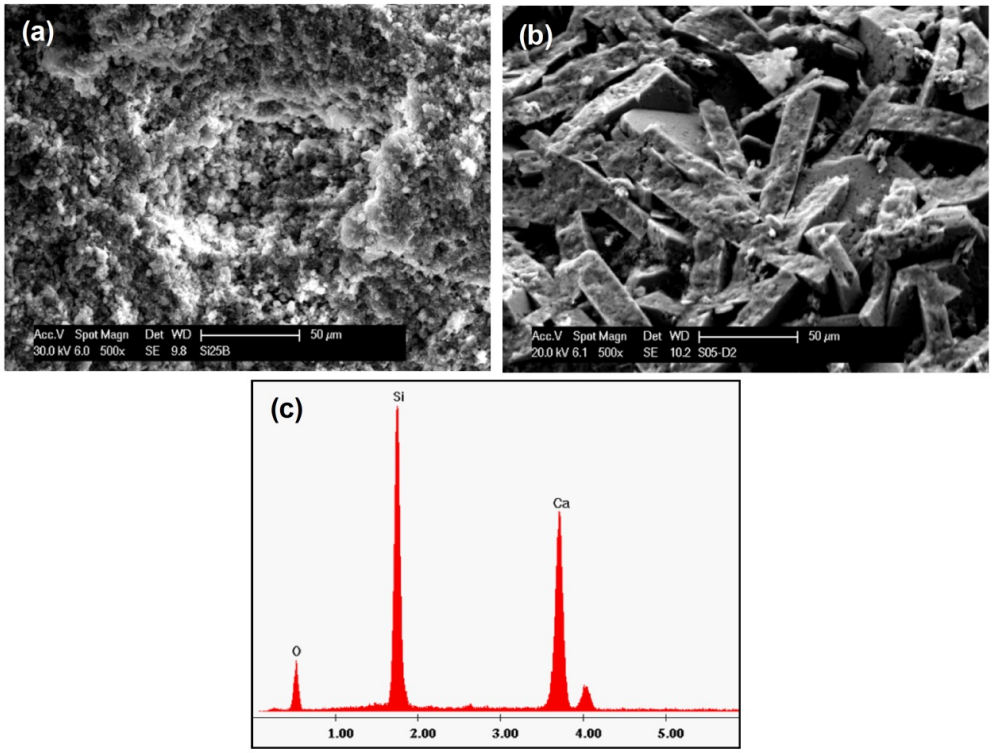

Figure 8. The micrographs of the cross sections of (a) SiO_2 pellet sintered at 1573 K for 3 h before electrolysis (b) The intermediate region of the pellet electrolysed $CaCl_2$ melt rich in $CaSiO_3$ and (c) the corresponding EDX spectrum.

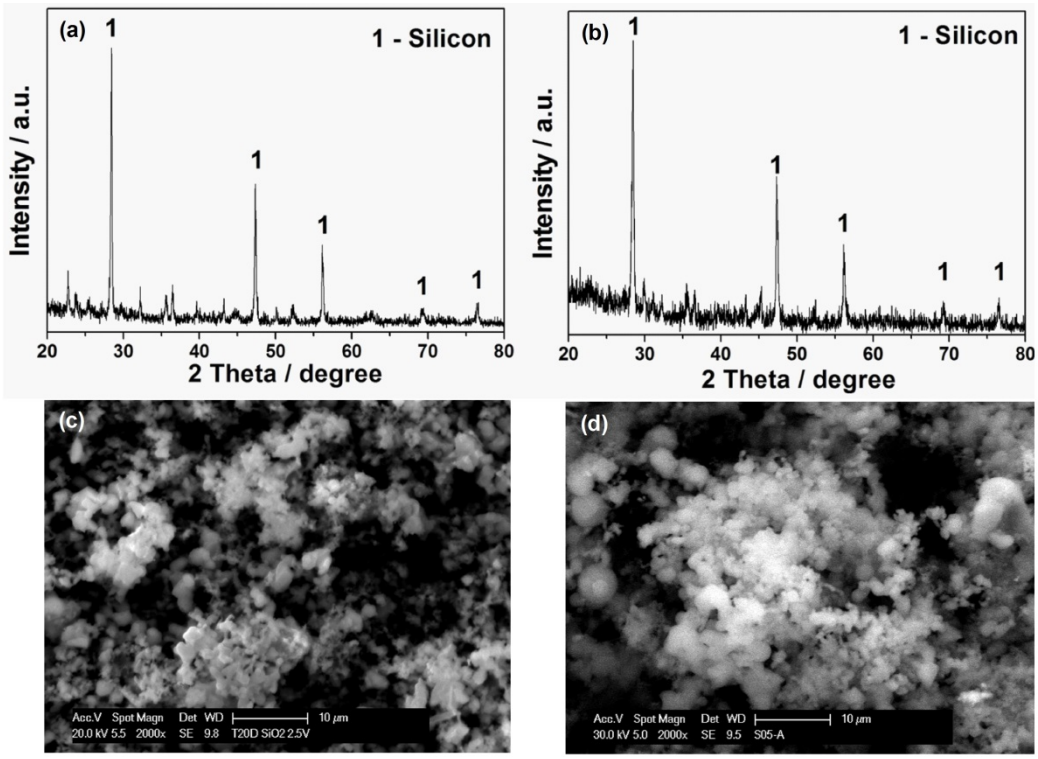

Figure 9. X-ray diffraction patterns of Si produced from electrolysis at (a) 2.5 V and (b) 2.8 V in $CaCl_2$ melt at 1173 K. The scanning electron micrographs of silicon from (a) and (b) are given in (c) and (d), respectively.

The morphology of Si produced in both the cases was similar and contained particles of Si ranging from tens of nm to μm. The highly porous structure of the produced Si during electrolysis of SiO_2 in fully dipped condition would have allowed the removal of the released oxide ions from the reaction interface in to the bulk of the melt rather quickly and led to faster reduction. However, in case of electro-reduction in tip dipped condition, the reduction zone is surrounded by limited

e-ISSN: 2321-6212
p-ISSN: 2347-2278

quantity of $CaCl_2$ electrolyte, which is facilitated by the capillary action of the melt along the pellet from the dipped tip to the reduction zone. Therefore the released oxide ions are available in the vicinity of the reduction zone and react chemically with the adjacent unreduced SiO_2 particles in the presence of Ca^{2+} ions to form $CaSiO_3$ ($Ca^{2+} + SiO_2 + O^{2-} \rightarrow CaSiO_3$). Since Si is highly porous and would aid easy removal of the generated oxide ions away from the reaction site in the fully dipped condition, $CaSiO_3$ was not observed as an intermediate product during the electrochemical reduction of SiO_2 pellets [17,19-21,23-25,27].

Current Behaviour of TiO_2 and SiO_2 during Electrolysis

The I-t curves obtained for electrolysis of two TiO_2 pellets (weight 1.5 g each, 1.5 mm thick, 21 mm dia., sintered at 1573 K for 3 h, open porosity ~20%), one configured as in **Figure 1a** and the other as in **Figure 1b**, in $CaCl_2$ melt at a constant applied voltage of 3.1V are shown in **Figure 3**. The current behaviour of a cell with SiO_2 pellet in the similar two configurations is given in **Figure 10**.

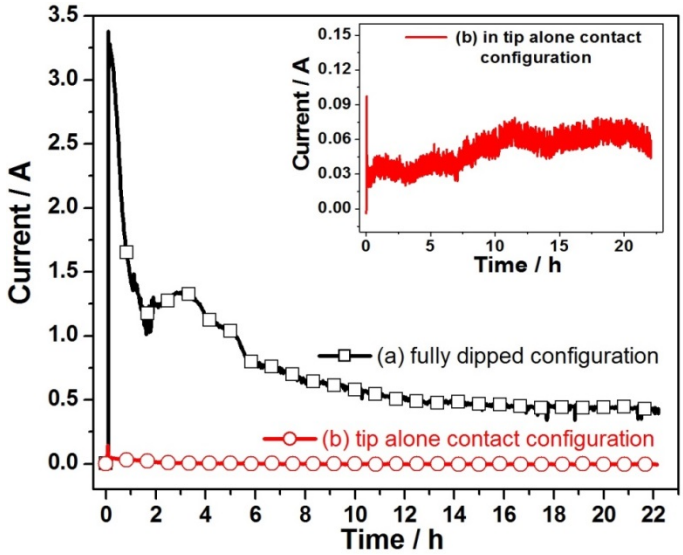

Figure 10. The variation of current with time during electro-reduction of SiO_2 pellets in (a) fully dipped configuration and (b) in the tip alone contact configuration in $CaCl_2$ melt at 1173 K. Inset shows the magnified version of beginning part of graph (b), which shows the slow increase of current in the later case with duration of electrolysis.

The current in an electrodeoxidation cell is mainly due to the transport of the cathodically generated O^{2-} ions and the cell current is directly related to the electroactive area of the oxide electrode. The shape of the electrolysis curves of the TiO_2 electrode (a high current in the beginning which decreases with time), therefore, shows that the electroactive area of the oxide electrode was maximum at the start of the experiment and it decreased with time as electrolysis was continued. This in other words meant that the maximum area of the TiO_2 pellet was electronically conducting in the beginning of electrolysis itself. It can be seen that the current behaviour of both the cells with 'tip dipped' and 'fully dipped' TiO_2 pellet cathodes is similar. This observation further shows that the oxide electrode was good conducting throughout its body, irrespective of the location of the current lead, and followed the 2PI mechanism of reduction as discussed previously.

The shape of the electrolysis curves of the two cells with SiO_2 pellet in the two different configurations (**Figure 1a and 1b**), obviously, presents a different picture. Unlike the TiO_2 cell, the cell current is low in the beginning of electrolysis and it slowly increased with time as electrolysis was continued. This typical current behaviour of SiO_2 electro-deoxidation cells was reported by many investigators too in the past. Obviously, the electroactive area of the electrode increased with time during the course of electrolysis. In the beginning of electrolysis, due to poor electronic conduction, the SiO_2 pellet could become electrochemically active only at those points on the electrode where the metal lead wire was in contact and the electroactive area and hence current increased as the electro-generated silicon particles acted as electron conducting bridges to the adjoining oxide particles. The typical current behaviour of SiO_2 electrode, unlike that of TiO_2 electrode, is a valid proof of the need of a solid electron conductor for supplying electrons to the insulating SiO_2 oxide particle at the reaction interface for its electroreduction to occur.

CONCLUSION

The results of the novel electrochemical deoxidation experiments carried out with electrically insulating SiO_2 and electrically conducting TiO_2 pellet electrodes in high-temperature $CaCl_2$ melt, presented in this study, clearly show that

the propagation of the electro-deoxidation through the solid oxide matrices and hence the physical nature of deoxidation of the two oxides are related to their electron conducting property. In the case of solid SiO_2 electrode, as reported earlier by Nohira et al. [32], the reduction reaction was initiated only at those locations where the electron conducting lead metal wire was in close physical contact with the oxide electrode, showing thereby the need for co-existence of the three physically distinct phases, viz. the solid electron conductor, the solid oxide, and the liquid electrolyte (3 PI) for deoxidation of the electrically insulating oxide to occur. However, the reduction of the tip of a TiO_2 electrode, where no solid electron conductor is in contact with the oxide, clearly shows that the oxide electrode allowed passage of electrons from the metal lead wire through it and thus made available electrons at the solid oxide/liquid electrolyte melt interface for the deoxidation reaction. Obviously, two physically distinct phases, viz. the solid oxide and liquid electrolyte melt phases (2PI) were only present at the reaction interface. The 3PI mechanism, proposed to explain the electrodeoxidation of insulating SiO_2 [28,32,33], is thus demonstrated to stand reduced to 2 PI mechanism in the case of the conducting TiO_2 electrode, in this study. It is also shown here that electro-active area and hence the current of the oxide electrode, which is deoxidised in the 2 PI mechanism (TiO_2) decreases with passage of time where as the opposite happens in the case of an oxide electrode like SiO_2, which follows the 3PI mechanism of electrodeoxidation.

ACKNOWLEDGEMENTS

Sri Maha Vishnu D acknowledges the grant of the research fellowship from IGCAR, Department of Atomic Energy, India. The authors sincerely acknowledge the support of Dr. G. Panneerselvam in recording the X-ray diffractograms of the samples and Mrs. Soja K. Vijay for residual oxygen analysis of the samples. Thanks are due to Mr. V. Arun Kumar for his help during some of the experiments.

REFERENCES

1. Fray DJ, et al. Removal of oxygen from metal oxides and solid solutions by electrolysis in a fused salt, 1999, International patent no. WO 9964638.
2. Mohandas KS and Fray DJ. FFC Cambridge process and removal of oxygen from metal oxygen systems by molten salt electrolysis: An overview. Trans Indian Inst Met 2004;57:579.
3. Mohandas KS. Direct electrochemical conversion of metal oxides to metal by molten salt electrolysis: a review. Trans Inst Min Metall C 2013;122:197.
4. Chen GZ, et al. Direct electrolytic preparation of chromium powder. Metall Mater Trans 2004;35:223.
5. Mohandas KS and Fray DJ. Novel electrochemical measurements on direct electro-deoxidation of solid TiO_2 and ZrO_2 in molten calcium chloride medium. J Appl Electrochem. 2011;41:321-336.
6. Sri Maha Vishnu D. Studies on the molten salt electro-deoxidation of niobium, titanium, silicon and uranium oxides. Ph.D dissertation. Homi Bhabha National Institute, Mumbai, India. December 2013.
7. Sri Maha Vishnu D, et al. A study of the reaction pathways during electrochemical reduction of dense Nb_2O_5 pellets in molten $CaCl_2$ medium. Electrochim Acta 2013;100:51-62.
8. Bixia W, et al. Cathode preparation of electrochemical reduction process of TiO_2 to titanium. Rare Metal Mat Eng 2010;39:1513-1518.
9. Schwandt C and Fray DJ. Determination of the kinetic pathway in the electrochemical reduction of titanium dioxide in molten calcium chloride. Electrochim Acta 2005;51:66-76.
10. Chen GZ, et al. Direct electrochemical reduction of titanium dioxide to titanium in molten calcium chloride. Nature 2000;407:361-364.
11. Sri Maha Vishnu D, et al. Electrochemical reduction of TiO_2 powders in molten calcium chloride. Electrochim. Acta 2015;159:124-130.
12. Yan XY, Fray DJ. Production of niobium powder by direct electrochemical reduction of solid Nb_2O_5 in a eutectic $CaCl_2$-NaCl melt. Metall Mater Trans B 2002;33B:685-693.
13. Sri Maha Vishnu D, et al. Electrochemical conversion of solid Nb_2O_5 to Nb in sodium chloride melt as proof of oxygen ionisation mechanism of electrodeoxidation. J Alloys Compd 2016;677:258-265.
14. Sri Maha Vishnu D, et al. Mechanism of direct electrochemical reduction of solid UO_2 to uranium metal in $CaCl_2$-48 mol% NaCl melt. J Electrochem Soc 2013;160:D394-D402.
15. Sri Maha Vishnu D, et al. Determination of the extent of reduction of dense UO_2 cathodes from direct electrochemical reduction studies in molten chloride medium. J Nucl Mater 2012;427:200-208.

16. Sri Maha Vishnu D, et al. Factors influencing the direct electrochemical reduction of UO_2 pellets to uranium metal in $CaCl_2$-48 mol% NaCl melt. J Electrochem Soc 2013;160:D583-D592.
17. Yasuda K, et al. Mechanism of direct electrolytic reduction of solid SiO_2 to Si in molten $CaCl_2$. J Electrochem Soc 2005;152:D69-D74.
18. Yasuda K, et al. Diagrammatic representation of direct electrolytic reduction of SiO_2 in molten $CaCl_2$. J Electrochem Soc 2007;154:95-101.
19. Yasuda K, et al. Electrolytic reduction of a powder-molded SiO_2 pellet in molten $CaCl_2$ and acceleration of reduction by Si addition to the pellet. J Electrochem Soc 2005;152:D232-D237.
20. Nishimura Y, et al. Formation of Si nanowires by direct electrolytic reduction of porous SiO_2 pellets in molten $CaCl_2$. J Electrochem Soc 2011;158:E55-E59.
21. Cho SK, et al. Formation of a silicon layer by electroreduction of SiO_2 nanoparticles in $CaCl_2$ molten salt. Electrochim Acta 2012;65:57-63.
22. Xiao W, et al. Rationalisation and optimisation of solid state electro-reduction of SiO_2 to Si in molten $CaCl_2$ in accordance with dynamic three-phase interlines based voltammetry. J Electroanal Chem 2010;639:130-140.
23. Nohira T, et al. Pinpoint and bulk electrochemical reduction of insulating silicon dioxide to silicon. Nat Mater 2003;2:397-401.
24. Ergul E, et al. Electrochemical decomposition of SiO_2 pellets to form silicon in molten salts. J Alloy Compd 2011;509:899-903.
25. Yasuda K, et al. Effect of electrolysis potential on reduction of solid silicon dioxide in molten $CaCl_2$. J. Phys Chem Solids 2005;66:443-447.
26. Jin X, et al. Electrochemical preparation of silicon and its alloys from solid oxides in molten calcium chloride Angew Chem 2004;116:751-754.
27. Yasuda K, et al. Direct electrolytic reduction of solid SiO_2 in molten $CaCl_2$ for the production of solar grade silicon. Electrochim Acta 2007;53:106-110.
28. Chen GZ, et al. Direct electrolytic preparation of chromium powder. Metall Mater Trans B 2004;35B:223-233.
29. Xiao W and Wang D. The electrochemical reduction processes of solid compounds in high temperature molten salts. Chem Soc Rev 2014;43:3215-3228.
30. Xiao W, et al. Electrochemically driven three-phase interlines into insulator compounds: Electroreduction of solid SiO_2 in molten $CaCl_2$. Chem Phys Chem 2006;7:1750-1758.
31. Jin XB, et al. Electrochemical preparation of silicon and its alloys from solid oxides in molten calcium chloride. Angew Chem Int Ed 2004;43:733-736.
32. Deng Y, et al. Electrochemistry at conductor/insulator/electrolyte three-phase interlines: A thin layer model. J Phys Chem B 2005;109:14043-14051.
33. Wang D, et al. Solid state reactions: an electrochemical approach in molten salts. Annu Rep Prog Chem Sect C 2008;104:189-234.
34. Massalski TB. Ti-O phase diagram. In: Massalski TB. Binary alloy phase diagrams (2^{nd} edn). ASM Int 1990;3:2941.
35. Song HS, et al. Effect of microstructural features on the electrical properties of TiO_2. Mat Sci Eng 2002;B94:40-47.
36. Bak T, et al. Electronic and ionic conductivity of $CaTiO_3$. Ionics 2004;10:334-342.
37. Okamoto H. O-Si phase diagram. J Phase Equilib Diff 2007;28:309-310.
38. Srivastava JK, et al. Electrical conductivity of silicon dioxide thermally grown on silicon. J Electrochem Soc 1985;132:955-963.